



LAWRENCE  
LIVERMORE  
NATIONAL  
LABORATORY

# Gamma ray mirror experimental campaign at INL's ZPPR facility: Preliminary report

J. Ruz-Amendariz, N. Brejnholt, T. Deckker, R. Hill, M.  
A. Descalle, M. Pivovarovoff, K. Ziock, D. Chichester, S.  
Watson

January 12, 2015

## **Disclaimer**

---

This document was prepared as an account of work sponsored by an agency of the United States government. Neither the United States government nor Lawrence Livermore National Security, LLC, nor any of their employees makes any warranty, expressed or implied, or assumes any legal liability or responsibility for the accuracy, completeness, or usefulness of any information, apparatus, product, or process disclosed, or represents that its use would not infringe privately owned rights. Reference herein to any specific commercial product, process, or service by trade name, trademark, manufacturer, or otherwise does not necessarily constitute or imply its endorsement, recommendation, or favoring by the United States government or Lawrence Livermore National Security, LLC. The views and opinions of authors expressed herein do not necessarily state or reflect those of the United States government or Lawrence Livermore National Security, LLC, and shall not be used for advertising or product endorsement purposes.

This work performed under the auspices of the U.S. Department of Energy by Lawrence Livermore National Laboratory under Contract DE-AC52-07NA27344.

# Gamma ray mirror experimental campaign at INL's ZPPR facility: Preliminary report

Jaime Ruz-Armendariz, Nicolai Brejnholt, Randy Hill, Todd Decker, Marie-Anne Descalle, Mike Pivovarov, (LLNL)

Klaus Ziock,(ORNL)

David Chichester, Scott Watson(INL)

Unclassified

December 1, 2014

## **Disclaimer**

This document was prepared as an account of work sponsored by an agency of the United States government. Neither the United States government nor Lawrence Livermore National Security, LLC, nor any of their employees makes any warranty, expressed or implied, or assumes any legal liability or responsibility for the accuracy, completeness, or usefulness of any information, apparatus, product, or process disclosed, or represents that its use would not infringe privately owned rights. Reference herein to any specific commercial product, process, or service by trade name, trademark, manufacturer, or otherwise does not necessarily constitute or imply its endorsement, recommendation, or favoring by the United States government or Lawrence Livermore National Security, LLC. The views and opinions of authors expressed herein do not necessarily state or reflect those of the United States government or Lawrence Livermore National Security, LLC, and shall not be used for advertising or product endorsement purposes.

Lawrence Livermore National Laboratory is operated by Lawrence Livermore National Security, LLC, for the U.S. Department of Energy, National Nuclear Security Administration under Contract DE-AC52-07NA27344.

## Table of Contents

<b>1</b>	<b>Introduction</b>	<b>1</b>
<b>2</b>	<b>Experiment</b>	<b>2</b>
2.1	Plutonium source	2
2.2	Multilayer mirror	2
2.3	2D HPGe detector	3
2.4	Experimental set-up	3
2.5	Data Analysis/Post-processing	4
<b>3</b>	<b>Results</b>	<b>4</b>
3.1	Beam characterization	4
3.2	Americium rocking curve	5
3.3	Plutonium emission lines	7
<b>4</b>	<b>Simulations</b>	<b>9</b>
4.1	Ray Tracing	9
4.2	Monte Carlo Simulations	9
<b>5</b>	<b>Summary</b>	<b>11</b>
	<b>References</b>	<b>11</b>

# Gamma ray mirror experimental campaign at INL's ZPPR facility

## Preliminary report

### 1 Introduction

The Next Generation Safeguard Initiative (NGSI) spent fuel non-destructive assay (NDA) project is part of the United States effort established in response to the needs of the international safeguards community and its primary goal is to develop technologies for the direct and independent quantification of Pu mass in spent fuel with an uncertainty of more than 5%.[1]

Direct measurements of gamma rays emitted by fissile material are a desirable alternative since it does not rely on inference from measurements of the gamma rays from fission products. From a safeguards applications perspective, direct detection of uranium (U) and plutonium (Pu) K-shell fluorescence emission lines and isotope-specific lines from  $^{235}\text{U}$ ,  $^{238}\text{Pu}$ ,  $^{239}\text{Pu}$ ,  $^{240}\text{Pu}$ , and  $^{241}\text{Pu}$  could lead to improved shipper-receiver difference or input accountability at the start of Pu reprocessing. [2, 3] However, these measurements are difficult to implement when the spent fuel is in the line-of-sight of the detector, as the detector is exposed to an intense radiation field dominated by the high activity of fission products compared to that of U and plutonium Pu.

To overcome the combination of high rates and high background, we propose the use of grazing incidence multilayer mirrors to selectively divert hard X-ray and soft gamma rays in the 90 to 420 keV energy band of U and Pu emission lines into a high-purity germanium (HPGe) detector shielded from the line-of-sight radiation from spent fuel. Several groups demonstrated that K-shell fluorescence lines of U and Pu from spent fuel could be detected with Ge detectors.[3, 6] In the field of hard X-ray optics the performance of reflective multilayer coated reflective optics was demonstrated up to 645 keV at the European Synchrotron Radiation Facility.[7-9]. Initial measurements conducted at Oakridge National Laboratory with sealed sources and scoping experiments with spent nuclear fuel conducted at the ORNL Irradiated Fuels Examination Laboratory (IFEL) further demonstrated the pass-band properties of multilayer mirrors for reflecting specific emission lines into a 1D or 2D HPGe.[10, 11].

Although the long term goal of the LLNL gamma ray mirror system program is NDA of Pu in spent nuclear fuel, stringent experimental conditions with a well-defined Pu source in a low background environment were required to evaluate the detection system characteristics. This report summarizes preliminary results from an

experimental campaign conducted at Idaho National Laboratory (INL) zero power physics reactor (ZPPR) to demonstrate the efficacy of gamma ray multilayer mirrors as a pass-band filter for reflecting Pu isotope-specific emission lines into an imaging HPGe detector.

## 2 Experiment

The experiment was conducted in INL's ZPPR cell from September 22 to 26, 2014. The reader is referred to the INL report for details regarding the facility. One of the key advantages of the ZPPR cell is a low and well-documented background.[12] K-shell fluorescence lines and gamma emission lines from a plutonium source were reflected by a flat multilayer coated mirror into a gamma imaging germanium detector.

### 2.1 Plutonium source

The source was a legacy plutonium fuel plate with high  $^{240}\text{Pu}$  content from the former ZPPR program of dimensions 3.2 mm x 2.54 cm x 7.62 cm.[12] Its composition is given in table 1.

Table 1 High  $^{240}\text{Pu}$ -content fuel plate composition on September 22, 2014. Values are decay corrected.[12]

Isotope	$^{238}\text{Pu}$	$^{239}\text{Pu}$	$^{240}\text{Pu}$	$^{241}\text{Pu}$	$^{242}\text{Pu}$	$^{241}\text{Am}$
Weight [g]	0.0002	79.691	23.921	0.673	0.671	4.247
Half-life [y]	87.74±0.04	24,119±26	6564±11	14.348±0.022	376,300±900	433.6±1.4

### 2.2 Multilayer mirror

The physics of multilayer optics has been described in details in previous publications. [7-11]

The X-ray mirror consisted of a single flat highly-polished fused silica substrate with dimensions 150 mm x 150 mm x 6.4 mm coated with tungsten carbide (WC)/silicon carbide (SiC) multilayers made of N=300 bilayers with a nominal period thickness  $d=15.2 \text{ \AA}$ . (see figure 1) The mirror has been extensively characterized at 0.8 and 8 keV and its response is well-understood up to 645 keV.[7-9]

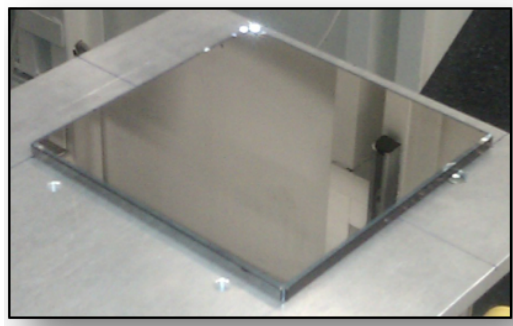


*Figure 1. WC/SiC Multilayer mirror*

### 2.3 2D HPGe detector

Gamma spectra and images were recorded with a gamma ray imaging detector, or GeGI (PHDS Co., Knoxville, TN). The GeGI is a 173 x 173 pixels position-sensitive, mechanically cooled HPGe detector with a 1cm-thick by 9 cm-diameter crystal. Each pixel has an effective area of 520 x 520  $\mu\text{m}^2$  and records an energy spectrum between 0 and 2048 keV in 0.5 keV wide bins. The stated energy resolution is better than 2.1 keV at 662 keV.[13]

### 2.4 Experimental set-up

To reduce background contributions in the detector, a two-slit collimation system was built with copper bricks 2.54 cm x 10.16 cm x 15.24 cm. The rectangular slit closest to the source was 3.175 mm wide while the narrow exit slit was 250  $\mu\text{m}$  wide. In addition, the detector was enclosed in a lead housing, The mirror was in a vertical position to limit gravity effects. The mirror angle relative to the line of sight between the detector and the collimated fuel plate was set prior to each measurement. The source collimator and the mirror system are shown in figure 2, and the experimental set up is shown in figure 3.

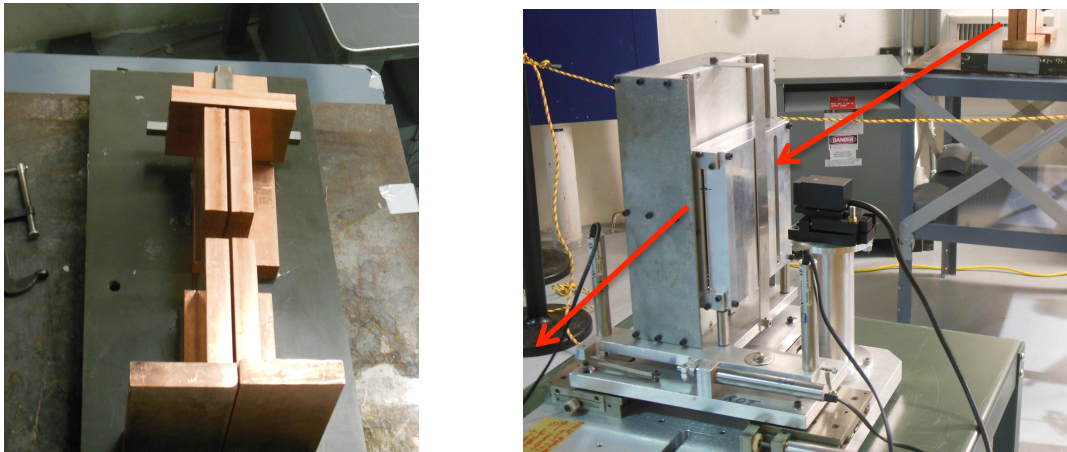


*Figure 2. Detail of the experimental set-up: left) copper collimator, the fuel plate (not visible) is held by the two plates at the top of the image; right) multilayer mirror, collimator and stage. The red arrow indicate the path the gamma-ray photons.*

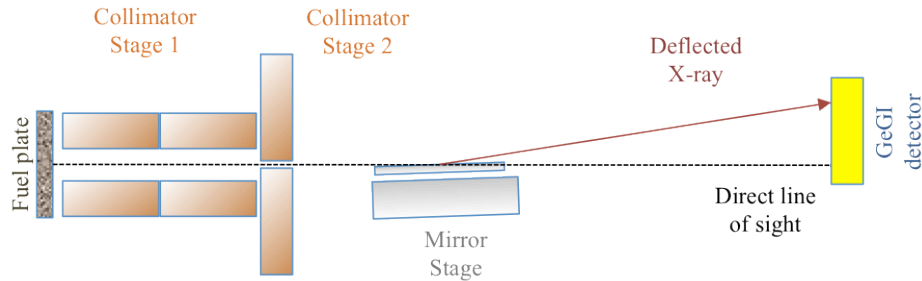


Figure 3. Top View of the source collimation, stage and mirror systems and detector.

## 2.5 Data Analysis/Post-processing

The data generated by the HPGe detector, or  $173 \times 173$  pixels  $\times$  4096 integers, was processed with an in-house C++ and ROOT based code to generate intensity maps, integrated counts and energy spectra summed over a band of pixels. In addition spectral filtering around lines of interest can be easily applied. For example, nominally, intensity maps represent integrated counts in each pixel in the energy range 0 to 2048 keV, but an intensity map of the 59.54 keV americium line can be generated by applying a 57 to 61 keV energy window.

## 3 Results

### 3.1 Beam characterization

To characterize the nature and size of the direct beam at the mirror location, the HPGe detector was first centered on the collimator axis and set 2.36 m from the source without the mirror structure in place. As shown in figure 4 the beam was 25 mm wide along the x-axis and filled the detector active surface along the y-axis. The detector was then shifted laterally to an intermediate position 20 mm from the initial centered position to check the detector response was independent of the position at which the image is generated. The latter setup enables the detection of both direct beam and reflected lines once the detector is moved back to the desired position about 4 m from the mirror.

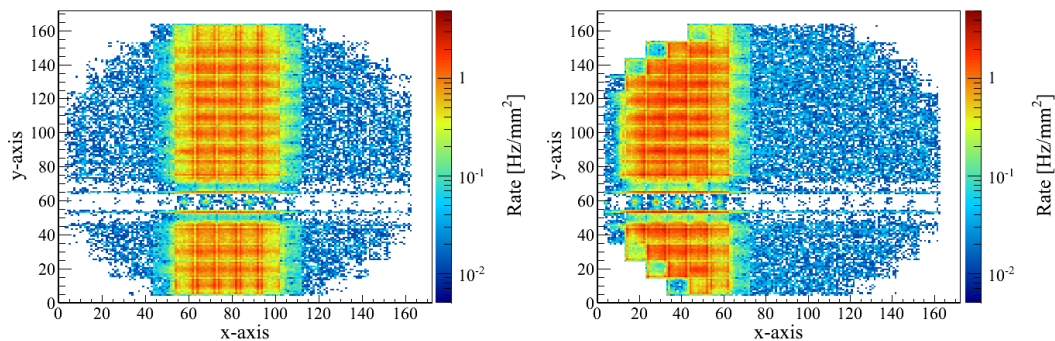


Figure 4. Images of the beam recorded with the HPGe position-sensitive detector at the mirror location: left) the detector was centered on the collimator axis and right) the detector was shifted laterally with respect to the collimator axis. Numbers on the x-

and  $y$ -axis represent pixel numbers. A band of defective pixels can be seen in the lower part of the image from  $y$ -pixel position 45 to 70.

Spectra of photon rates were summed over all illuminated pixels for each detector position and are compared in figure 5. They are very similar even though the beam illuminates different regions of the detector: they both exhibit a prominent peak around 59 keV corresponding to the americium line and low peaks in the 100 keV range, a range in which several Pu lines can be found. At energies above 70 keV the spectrum of the off center beam is slightly lower.

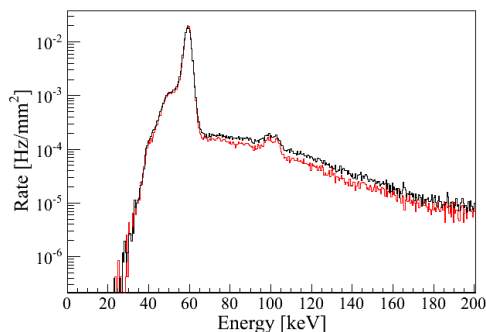


Figure 5. Spectra summed over all high intensity pixels for a centered detector (red) and for a detector with lateral offset (black).

### 3.2 Americium rocking curve

The mirror stage was positioned such that the center of the mirror was 2.084 m from the front of the fuel sample. The HPGc detector was set back 4.3254 m from the center of the mirror, or 6.410 m from the source, to minimize scattered photon contributions and to clearly split the direct beam from the deflected photons. In this configuration, the direct beam can be seen as a wide band between pixel  $x$ -position 10 to 30.

The performance of our setup can be quantified by comparing the measured angle of the mirror relative to the incident beam to the expected value defined by Bragg's law. Measurements were obtained for 6 mirror angles in increments of 30 arcsec. Figure 6 shows intensity maps in the 57 to 61 keV energy range around the 59.54 keV Americium line.

The rocking curve plotted in figure 7 was obtained from data shown in figure 6 by integrating counts over all illuminated pixels in the energy band encompassing the deflected Am line, i.e. between  $x$ -pixel number 120 to 140 and  $y$ -pixels number 10 to 172. The rocking curve was fitted with a second order polynomial as expected from theory and, the maximum was at an angle of 1454 arcsec.

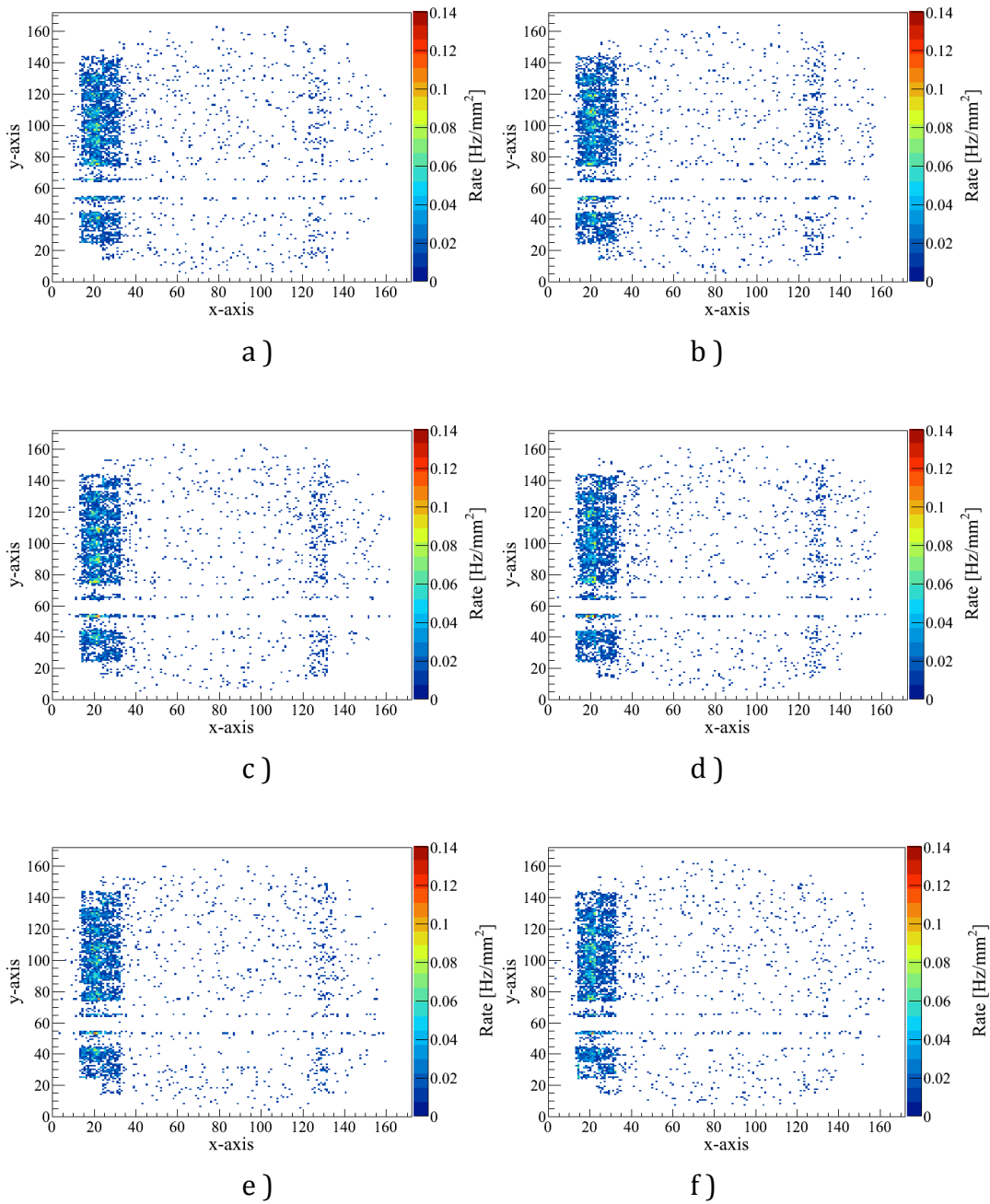


Figure 6. Intensity maps in the 57-61 keV energy range at 6 mirror angles. Angle settings in arcsec were a) 1362, b) 1392, c) 1422, d) 1452, e) 1482, and f) 1512 once corrected for offset. The narrow vertical band on the right of each image corresponds to the reflected 59.54 keV americium line.

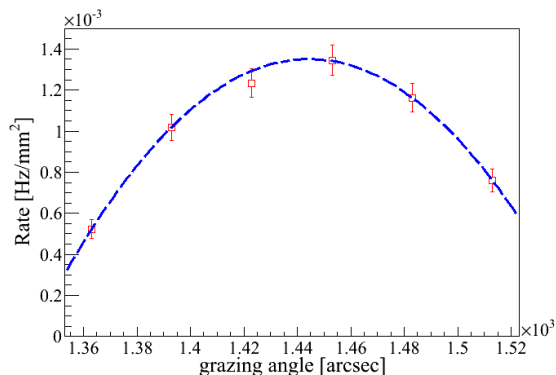


Figure 7. Rocking curve for the 59.54 keV americium line.

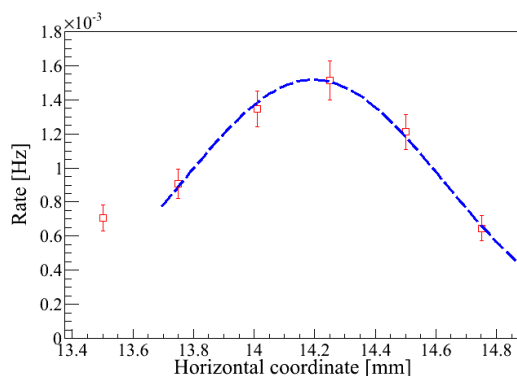


Figure 8. Total intensity in the ROI corresponding to the deflected americium line for 6 stage positions. The mirror angle was set to 1454 arcsec, the maximum of the rocking curve, and the stage was stepped horizontally.

Finally, to check if the maximum beam intensity corresponded to the maximum of the rocking curve, the mirror stage was stepped horizontally in increments of 250  $\mu\text{m}$  as shown in figure 8. The peak intensity was observed at a position of  $\sim 14.2$  mm, while the rocking curve shown in figure 7 was obtained for a horizontal stage position of 14.01, or a 10% loss relative to the maximum intensity.

### 3.3 Plutonium emission lines

To verify emission lines were homogeneously distributed over the beam, an energy window between 98 and 112 keV was applied to the direct beam data shown in figure 4 left. Figure 9 shows a homogeneous distribution within the collimated beam. Within the region of interest defined by the beam and excluding non-working y-pixels 40 to 70, the calculated mean flux in the 98 to 112 keV range was  $4.2 \times 10^{-3}$  photons/ $\text{mm}^2$  at the mirror stage.

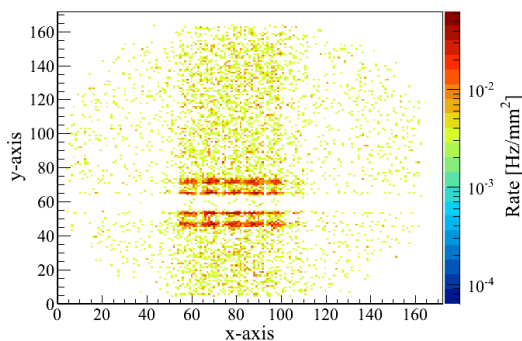


Figure 9. Intensity map in 98-112 keV energy range. The detector was 2.36 m from the source and centered on the beam.

The mirror angle was set to 840 arcsec to reflect lines in the 100 keV range and the detector was repositioned 6.410 m from the source. Data were acquired for  $10^4$  s. Reflected lines between 98 and 112 keV should be visible between x-pixels position 83 to 104. Unfortunately, except for a faint signal due to the direct beam between x-pixels numbers 0 to 35, the intensity map in figure 10 does not exhibit any structure raising two possibilities: either there were no photons of  $\sim 100$  keV reflected by the mirror or the signal was masked by background.

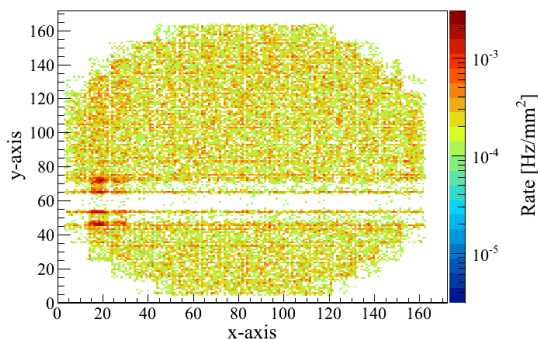


Figure 10. Intensity map of 100 keV lines for the mirror tilt angle set to 840 arcsec.

Several parameters must be taken into account when calculating the number of photons that should be deflected, namely the beam flux, the mirror dimensions and its angular tilt. The mirror area is  $150 \times 150 \text{ mm}^2$ , and the tilt in the y-axis is 840 arcsec to deflect  $\sim 100$  keV photons, the effective beam surface for deflection is  $0.62 \times 150 \text{ mm}^2$ , and the detector height is 90 mm. The effective beam area deflecting to our detector is roughly  $56 \text{ mm}^2$  for a total flux of 0.24 deflected photons per second. Over  $10^4$  s, 2400 deflected photons will be distributed over  $20 \times 135$  pixels or 0.89 deflected photons per pixel while the overall mean background level per pixel is 1.46 photons in the same energy range. In conclusion, the background level per pixel was too high to resolve the deflected photons. It is worth noting the intensities of the deflected americium line shown in figure 6 were fairly weak despite the fuel plate strong americium activity.

In an effort to understand the differences between INL and ORNL measurements, their respective measured rate as a function of area were compared within the 100 keV energy range. The mean rate obtained from the INL data shown in figure 10 is  $3 \times 10^{-4}$  Hz/mm<sup>2</sup> and that of the ORNL data in figure 11 is  $4 \times 10^{-2}$  Hz/mm<sup>2</sup> over two orders of magnitude higher. Some of the possible contributing factors to the lack of signal observed in the INL data are the source activity and the effective area of the optic -the X-ray optics deployed at ORNL consisted of a stack of five 100 x 100 mm<sup>2</sup> mirrors, i. e. 2.2 times larger. An increase in collection area would allow to better resolve these low intensity lines, which could be enabled by a custom-built x-ray optic.

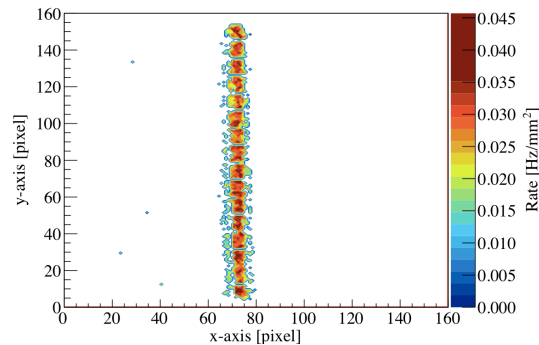


Figure 11. Intensity map at ~100 keV from ORNL/IFEL data

## 4 Simulations

### 4.1 Ray Tracing

Ray-tracing simulations of the X-ray optics are ongoing and results will be presented in the final report.

### 4.2 Monte Carlo Simulations

Initial simulations of the fuel plate leakage spectrum and the spectrum incident on the detector were performed with the MCNP5 Monte Carlo code to validate the basic model. [14] The source model consists of the line emission spectra for the high <sup>240</sup>Pu fuel plate simulated with radsrvc1.6 using input data from report INL/MIS-14-33068. [15] [12]. Details of the geometry and material composition can also be found in this report. It was inferred that the fuel had a density of 12.2 g/cm<sup>3</sup> and was contained within a 400 micron-thick stainless steel cladding. It is worth noting the high americium content of the source.

The simulated leakage spectrum of the fuel plate is shown in figure 18. The intensity of the 59.54 keV americium line is several orders of magnitude larger than the lines in the 100 keV range and several of the lines with significant intensity in the 100 keV region result from <sup>241</sup>Am decay.

In the first modeled experiment, the source is 10 cm from the front face of the detector and the source is shielded by a 0.5 cm thick copper plate to reduce low energy photon contributions in the detector. The photon spectrum incident on a 9 cm x 9 cm surface is tallied in 0.5 keV wide bins. The measured spectrum and simulated spectrum incident on the detector are shown in figure 19. While the main lines are clearly identifiable in both spectra, the shape of the spectra are significantly different, and notwithstanding missing details in the model, additional information regarding the detector energy resolution and efficiency are needed for a better comparison to measurements.

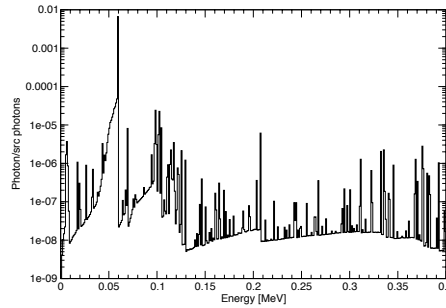


Figure 12. Simulated leakage spectrum for the high  $^{240}\text{Pu}$  fuel plate.

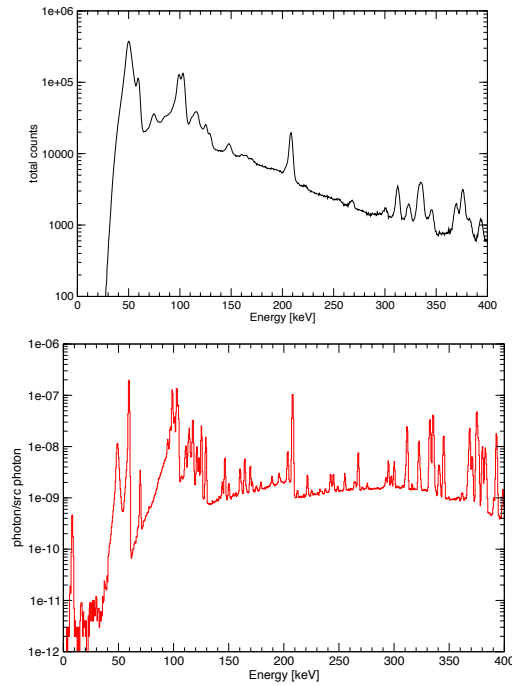


Figure 13. Measured spectrum in GeI detector (top) versus simulated spectrum incident on a 9 cm x 9 cm detector (bottom). The front face of the detector is located 10 cm from the source.

Ongoing simulation work aims at obtaining the photon flux and spectrum incident on the detector at the mirror location for exit slit widths of 250 microns and 3.175 mm respectively. These results will be useful for comparison to the estimated flux presented earlier.

## 5 Summary

Preliminary results from an experimental campaign conducted at INL ZPPR facility are presented in this report. The main goal was to demonstrate the efficacy of gamma ray multilayer mirrors as a pass-band filter for reflecting Pu isotope-specific emission lines into an imaging HPGe detector.

Although the results demonstrate that X-ray mirrors can act as filters for photons with energies in the band of interest for safeguards applications as demonstrated by the measurements of the 59.54 keV americium line, the lack of reflected Pu lines was in part related to a combination of source activity and low effective area of the prototype optics used. Simulations are ongoing to estimate the source spectrum incident on the detector.

This campaign highlighted several challenges from the competing need for both stringent requirements for precision alignment and for security procedures with respect to fissile material handling, to the need for an optic with a higher effective area. It is clear that the development of a dedicated larger effective area optics whether in the form of a flat stack or nested curved optics would result in significant increase in signal, and the implementation of a nested curved optics design would allow to focus photons on a smaller detector further increasing signal to noise ratio.

## References

1. M.Humphrey Non destructive assay of spent fuel for international safeguards. (<http://ramp.energy.gov/docs/education/Q17.pdf>), 2013(accessed20.05.13).
2. T. Hayakawa, et al., Nuclear Instruments and Methods A 621 695(2010).
3. A.S. Stafford, "Spent Nuclear Fuel Self-Induced XRF to Predict Pu to U Content," M.S. Thesis, Nuclear Engineering Texas A&M University, College Station, TX August 2010.
4. A.V. Bushuev, et al., Atomic Energy 53 (1982).
5. C. Rudy, P. Staples, K. Sereidnuik, and I. Yakovlev ,Determination of Pu in spent fuel assemblies by X-ray fluorescence, Proceedings of 46<sup>th</sup> Annual Meeting of the INMM, (2005).
6. W. S. Charlton et al. The use of self-induced XRF to quantify the Pu content in PWR spent nuclear fuel, Proceedings of the 31st Annual Meeting of ESARDA, (2009).

7. M. Fernandez-Perea, et al., Nuclear Instruments and Methods A 710 114(2013).
8. M. Fernandez-Perea, et al., Physics of reflective optics for the soft gamma-ray photon energy range, Physical Review Letters 111 027404 (2013).
9. N. Brejnholt, M.-A. Descalle, R. Soufli, M. Pivovarov, V. Honkimaki and F. Christensen, Optics Express (2014).
10. M. Pivovarov, K Zioc, M. Fernandez-Perea, M. Harrison, R. Soufli, Gamma-ray mirrors for direct measurement of spent nuclear fuel Nuclear Instruments and Methods in Physics Research A 743 109–113 (2014).
11. J. Ruz et al., Direct Measurement of <sup>235</sup>U in Spent Fuel Rods with Gamma-ray Mirrors, Submitted to Nuclear Instruments and Methods A, September 2014 (NIMA-D-14-00888).
12. D. Chichester, "Properties of nuclear fuel used in tests with the LLNL gamma ray mirror in September 2014". INL/MIS-14-33068 (2014).
13. <http://www.phdsco.com/>
14. Initial MCNP6 Release Overview, MCNP6 Beta 2. Los Alamos National Laboratory Report No. LA-UR-11-07082 (2011).
15. L. Hiller, T. Gosnell, J. Gronberg, D. Wright, Radsrc Library and Application manual UCRL-TM-229497 (2013).